

JOINT ESTIMATION OF MULTIPLICATIVE AND IMPULSIVE NOISE PARAMETERS IN REMOTE SENSING IMAGES WITH FRACTAL STRUCTURE

Mikhail Uss¹, Vladimir V. Lukin², Sergey Abramov², Benoit Vozel³, Kacem Chehdi³

¹ Dept of Radioelectronic Systems and Complexes, ² Dept of Receivers, Transmitters and Signal Processing, National Aerospace University 17 Chkalova Street, 61070, Kharkov, UKRAINE

Tel/fax + 38 057 3151186, E-mails uss@xai.edu.ua, luvin@xai.kharkov.ua

³ University of Rennes I, 6, Rue de Kerampont, 22 305 Lannion cedex, BP 80518, FRANCE,

Tel: +33 (0)2 96 46 90 71, Fax: 33 (0)2 96 46 90 75, E-mail Benoit.Vozel@enssat.fr

ABSTRACT

A novel approach to joint estimation of multiplicative noise variance and probability of impulsive noise occurrence in images is proposed. It uses a fractal Brownian motion model for description of real life images. It is demonstrated that this approach provides accurate estimation of mixed noise parameters even for images containing a large percentage of texture regions. The proposed method performance is compared to a modification of a recently designed method based on minimal inter-quantile distances.

Index Terms— Noise, Fractals, Parameter Estimation, Image Analysis, Image Restoration

1. INTRODUCTION

Airborne and satellite remote sensing (RS) complexes nowadays provide a lot of information useful for various applications [1]. But in practical situations different kinds of noise and distortions corrupt this information at stages of image forming and transmission. This leads to decreasing the reliability of RS data interpreting.

Knowing of noise and distortion type and characteristics allows selecting an appropriate image processing method. However, noise parameters are often unknown in advance. Moreover, they can vary in different image forming conditions. Thus, preliminary image analysis with the purpose of noise/distortion type and parameter determination is one of commonly used operations. To reduce the influence of subjective factors and to decrease RS images processing time, it is desirable to apply automatic estimation methods [2].

The methods described in [2] and [3] allow discriminating several complex noise/distortion situations. One among them typical for radar imaging [1] is a situation when an image is corrupted by mixed (multiplicative and impulsive) noise. Thus, below we consider the problem of joint estimation of parameters of such type of noise.

Note that there are quite many existing approaches to estimation of multiplicative and additive noise variance [4-6]. They are based on analysis and robust processing of a set of local variance estimates computed in scanning windows (SW). A general goal

was to provide applicability and appropriate accuracy of designed techniques for textural images.

However, the performance of these techniques quickly reduces if impulse noise is present in analyzed images and its probability is rather large [7]. Keep in mind that for many applications (especially, for image filtering [7]) it is strongly desirable to a priori know or to estimate the probability of impulsive noise (P_{imp}). Then it becomes necessary to design methods able to simultaneously estimate noise variance and P_{imp} . In available literature, we have not found any method dealing with blind estimation of P_{imp} . The only analog is the method proposed in our recent paper [8] that deals with blind estimation of mixed (additive and impulsive) noise parameters.

Thus, below we extend the approach [8] based on maximum likelihood estimation to the case of mixed multiplicative+impulsive noise. Moreover, to take into account the properties of real life RS images, we imply fractal Brownian motion (fBm) model that has become popular for describing many natural phenomena [9, 10].

2. OBSERVATION MODEL

Let us present an image as an $m_{\text{im}} \times n_{\text{im}}$ matrix denoted as \mathbf{x} . Let $x(t, s)$ denotes an element of matrix \mathbf{x} with coordinates (t, s) also called image pixel. For image description we propose to use a fBm model. By definition [10], fBm is a Gaussian process $W_{t,s}^H$ (original coordinates at the point $(0,0)$ - $W_{0,0}^H = 0$, $H \in [0,1]$) with correlation function

$$\langle W_{t,s}^H \cdot W_{t_1,s_1}^H \rangle = \frac{\sigma_x^2}{2} \left(\sqrt{t^2 + s^2}^{2H} + \sqrt{t_1^2 + s_1^2}^{2H} - \sqrt{(t-t_1)^2 + (s-s_1)^2}^{2H} \right), \quad (1)$$

where $\langle \cdot \rangle$ denotes ensemble expectation, σ_x^2 - is the variance of increment of fBm process on unit distance. To take into consideration heterogeneous structure of RS images we assume that fBm

Partly supported by the European Union. Co-financed by the ERDF and the Regional Council of Brittany, through the European Inter-reg3b PIMHAI project

parameters depend on spatial coordinates but in such a manner that within a small image fragment they can be treated as constant.

Image is supposed to be corrupted by a mixture of multiplicative and impulsive noise with unknown parameters. The observation model has the following form

$$y(t,s) = x(t,s) \cdot \eta^\mu(t,s); \quad \eta^\mu(t,s) \rightarrow N(1, \sigma_\mu^2), \quad (2)$$

$$z(t,s) = y(t,s) \cdot (1 - b_{\text{imp}}(t,s)) + n^i(t,s) \cdot b_{\text{imp}}(t,s), \quad (3)$$

$$P(b_{\text{imp}}(t,s) = 1) = P_{\text{imp}}, \quad P(b_{\text{imp}}(t,s) = 0) = 1 - P_{\text{imp}}, \quad (4)$$

where $t=1, 2, \dots, m_{\text{im}}, s=1, 2, \dots, n_{\text{im}}$, \mathbf{x} is the noise-free image, \mathbf{y} denotes the image corrupted by multiplicative noise, \mathbf{z} is the image corrupted by mixed multiplicative with (relative) variance σ_μ^2 and impulsive noise, η^μ denotes the matrix with normally distributed elements, b_{imp} is the binary random field (if $b_{\text{imp}}(t,s)=1$, then the pixel is corrupted by impulse, and otherwise), $n^i(t,s)$ - denotes random variables uniformly distributed in the range $[a, b]$. Pixel values of η^μ , b_{imp} and $n^i(t,s)$ are supposed to be spatially uncorrelated.

The problem is to estimate σ_μ^2 and the probability P_{imp} based on the observed field \mathbf{z} and taking into account aforementioned assumptions on statistical properties of noise-free image and noise.

3. ESTIMATION OF MIXED NOISE PARAMETERS

A general block diagram of the proposed approach (Fig 1) is practically the same as that one described in our earlier papers [8, 12]. At initialization step, preliminary impulse noise detection is performed using Abreu's method [11]. This algorithm has been chosen because of its simplicity and acceptable performance quality. As the result, a preliminary estimate $\hat{\mathbf{b}}_{\text{imp}}$ of the matrix \mathbf{b}_{imp} is obtained. Then, in further derivations we employ only those pixels that are not corrupted by detected impulses, i.e., the pixels with $\hat{b}_{\text{imp}}(t,s)=0$. The algorithm also needs initial values of mixed noise parameters. A good choice is to set them $\hat{\sigma}_\mu^2 = 0.01$ and $\hat{P}_{\text{imp}} = 5\%$.

At the first stage, fBm parameters' estimation in the SW is performed [13]. At the second stage, impulse noise filtering based on fBm parameters estimations and initial assumptions is carried out. The pixel values corrupted by impulses are predicted based on "uncorrupted" pixels within the SW [13]. At the third stage, more accurate detection of impulses is done with producing an improved estimate $\hat{\mathbf{b}}_{\text{imp}}$. The detection algorithm is the following

$$\hat{b}_{\text{imp}}(t,s) = \begin{cases} 1, & T(t,s) = (z(t,s) - \hat{x}_{\text{pr}}(t,s))^2 / \sigma_{z-x}^2 > T_0, \\ 0, & T(t,s) \leq T_0, \end{cases} \quad (5)$$

$$\text{where } \sigma_{z-x}^2 = (\hat{x}_{\text{pr}}(t,s) \cdot \hat{\sigma}_\mu)^2 + \sigma_{\text{pr}}^2(t,s) + \sigma_{\text{pr}}^2(t,s) \cdot \hat{\sigma}_\mu^2$$

$$T_0 = 2 \cdot \ln((b-a) \cdot (1 - \hat{P}_{\text{imp}}) / \hat{P}_{\text{imp}}) - \ln(2\pi \cdot \sigma_{z-x}^2),$$

$\hat{\sigma}_\mu^2$ is the estimation of σ_μ^2 formed at previous iteration, $\hat{x}_{\text{pr}}(t,s)$ is the central pixel value maximum likelihood prediction based on "uncorrupted" pixels within the SW, $\sigma_{\text{pr}}^2(t,s)$ is the variance of $\hat{x}_{\text{pr}}(t,s)$. $\hat{x}_{\text{pr}}(t,s)$ and $\sigma_{\text{pr}}^2(t,s)$ are derived at the second stage

according to algorithms given in [13].

Principle of impulse detector operation relies on assumption that for "uncorrupted" pixels a random value $z(t,s) - \hat{x}_{\text{pr}}(t,s)$ possesses Gaussian distribution $N(0, \sigma_{z-x}^2)$ (then $T(t,s)$ possesses χ^2 distribution with one degree of freedom). Strictly saying, it slightly differs from Gaussian but our studies have shown that this can be neglected. One advantage of the proposed detector that differs it from many known heuristic detectors [11] is an offered opportunity to determine false alarm rate P_{fa} . This particular property allows estimating P_{imp} .

Iterations stop when impulse noise detection results at previous and current iterations are identical (convergence condition). The first three stages are described in detail in [12] and [13]; here we concentrate on considering the fourth stage of σ_μ^2 and P_{imp} estimation. For simplicity, for all variables the indices corresponding to the iteration number are omitted.

For each pixel (t,s) , consider an $N_y \times 1$ sample \mathbf{Y} composed of "uncorrupted" pixels within $N \times N$ SW. Let \mathbf{X} denote the corresponding sample from the matrix \mathbf{x} . The true value of the central SW pixel is denoted as x_0 . An example of the sample \mathbf{Y} forming ($N=3$) is shown in Fig. 2 (the corrupted pixels are shown by black dots).

According to the chosen model of noise-free image, let us describe the sample \mathbf{X} as fBm-field with original coordinates in the SW center (that now corresponds to the point (0,0)) and with intensity bias equal to x_0 . Thus, $\mathbf{X} = \Delta\mathbf{X} + x_0$ where $\Delta\mathbf{X}$ is the unbiased fBm. Each SW position is characterized by a vector of parameters $\boldsymbol{\theta} = (\sigma_x(t,s), H(t,s), x_0)$. Omitting a constant that does not depend on $\boldsymbol{\theta}$, the likelihood function (LF) of \mathbf{Y} is

$$\ln L(\mathbf{Y}; \boldsymbol{\theta}) = -\frac{1}{2} \left[(\mathbf{Y} - x_0 \mathbf{1})^T \mathbf{R}_{\Delta\mathbf{X}}^{-1} (\mathbf{Y} - x_0 \mathbf{1}) + \ln(|\mathbf{R}_{\Delta\mathbf{X}}|) \right],$$

$$\text{where } R_{\Delta\mathbf{X}}(k,l) = \begin{cases} R_{\Delta\mathbf{X}}(k,l) + (R_{\Delta\mathbf{X}}(k,l) + x_0^2) \cdot \sigma_\mu^2, & k=l, \\ R_{\Delta\mathbf{X}}(k,l), & k \neq l, \end{cases}$$

$k, l = 1 \dots N_y$, \mathbf{I} is the $N_y \times N_y$ identity matrix, $\mathbf{R}_{\Delta\mathbf{X}}$ is correlation matrix of the vector $\Delta\mathbf{X}$ where $\mathbf{R}_{\Delta\mathbf{X}}$ is obtained according to (1). The score function $\boldsymbol{\Lambda} = \text{grad} \ln L(\mathbf{Y}; \boldsymbol{\theta})$, the Fisher information matrix $\mathbf{F} = \langle \boldsymbol{\Lambda} \cdot \boldsymbol{\Lambda}^T \rangle$ and the maximum likelihood estimate $\hat{\boldsymbol{\theta}}$ of $\boldsymbol{\theta}$ are derived at the first stage [13].

To estimate σ_μ^2 , we propose to use v different SWs placed uniformly on the image. The aggregate sample \mathbf{Y}_Σ consists of a set of samples \mathbf{Y}_i , $i = 1..v$, where each sample \mathbf{Y}_i consists of pixels for the i -th SW position. Aggregate vector of estimated parameters of size $(3 \cdot v + 1) \times 1$ has the form

$$\boldsymbol{\theta}_\Sigma = (\sigma_{x1}, H_1, x_{01}, \sigma_{x2}, H_2, x_{02}, \dots, \sigma_{xv}, H_v, x_{0v}, \sigma_\mu)^T.$$

The logarithmic LF for \mathbf{Y}_Σ is of the form

$$\ln L_\Sigma(\mathbf{Y}_\Sigma; \boldsymbol{\theta}_\Sigma) = \sum_{i=1}^v \ln L(\mathbf{Y}_i; \boldsymbol{\theta}_i).$$

Expressions for all elements of $\boldsymbol{\Lambda}_\Sigma = \text{grad} \ln L(\mathbf{Y}_\Sigma; \boldsymbol{\theta}_\Sigma)$ are derived at the first stage except of

$$\frac{\partial \ln L_{\Sigma}}{\partial \sigma_{\mu}} = -\frac{1}{2} \sum_{i=1}^v \left[(\mathbf{Y}_i - x_{0i} \mathbf{1})^T \frac{\partial \mathbf{R}_{\Delta \mathbf{Y}_i}^{-1}}{\partial \sigma_{\mu}} (\mathbf{Y}_i - x_{0i} \mathbf{1}) + \text{sp} \left(\frac{\partial \mathbf{R}_{\Delta \mathbf{Y}_i}}{\partial \sigma_{\mu}} \mathbf{R}_{\Delta \mathbf{Y}_i}^{-1} \right) \right],$$

where sp denotes spur, $\frac{\partial \mathbf{R}_{\Delta \mathbf{Y}_i}}{\partial \sigma_{\mu}} = 2\sigma_{\mu} (\text{diag}(\mathbf{R}_{\Delta \mathbf{Y}_i}) + x_{0i}^2 \cdot \mathbf{I})$.

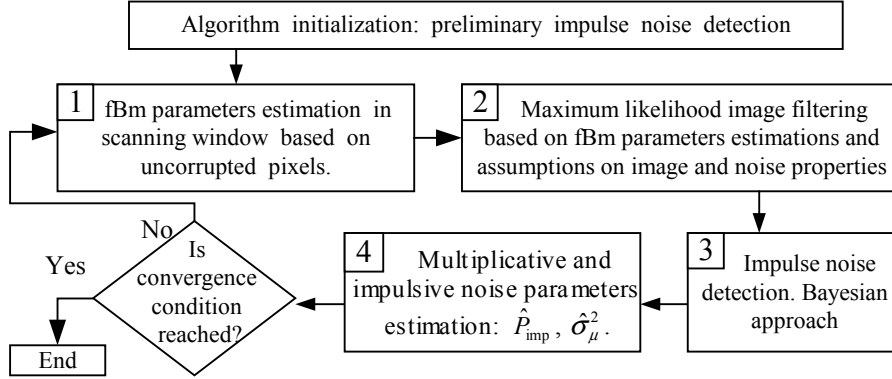


Fig. 1. Flow-chart of image corrupted by mixed noise filtering algorithm

The Fisher information matrix for \mathbf{Y}_{Σ} is expressed as

$$\mathbf{F}_{\Sigma} = \begin{pmatrix} \mathbf{F}_1 & 0 & \cdot & 0 & \mathbf{B}_1 \\ 0 & \mathbf{F}_2 & \cdot & 0 & \mathbf{B}_2 \\ \cdot & \cdot & \cdot & \cdot & \cdot \\ 0 & 0 & \cdot & \mathbf{F}_v & \mathbf{B}_v \\ \mathbf{B}_1^T & \mathbf{B}_2^T & \cdot & \mathbf{B}_v^T & \mathbf{E} \end{pmatrix}, \quad (6)$$

where \mathbf{F}_i is the Fisher information matrix for sample \mathbf{Y}_i ,

$$\mathbf{B}_i = -\frac{1}{2} \begin{pmatrix} \text{sp} \left(\frac{\partial \mathbf{R}_{\Delta \mathbf{Y}_i}}{\partial \sigma_{\mu}} \mathbf{R}_{\Delta \mathbf{Y}_i}^{-1} \frac{\partial \mathbf{R}_{\Delta \mathbf{Y}_i}}{\partial \sigma_{\mu}} \mathbf{R}_{\Delta \mathbf{Y}_i}^{-1} \right) \\ \text{sp} \left(\frac{\partial \mathbf{R}_{\Delta \mathbf{Y}_i}}{\partial H_i} \mathbf{R}_{\Delta \mathbf{Y}_i}^{-1} \frac{\partial \mathbf{R}_{\Delta \mathbf{Y}_i}}{\partial \sigma_{\mu}} \mathbf{R}_{\Delta \mathbf{Y}_i}^{-1} \right) \\ \text{sp} \left(\frac{\partial \mathbf{R}_{\Delta \mathbf{Y}_i}}{\partial x_{0i}} \mathbf{R}_{\Delta \mathbf{Y}_i}^{-1} \frac{\partial \mathbf{R}_{\Delta \mathbf{Y}_i}}{\partial \sigma_{\mu}} \mathbf{R}_{\Delta \mathbf{Y}_i}^{-1} \right) \end{pmatrix},$$

$$\mathbf{E} = -\frac{1}{2} \sum_{i=1}^v \left[\text{sp} \left(\frac{\partial \mathbf{R}_{\Delta \mathbf{Y}_i}}{\partial \sigma_{\mu}} \mathbf{R}_{\Delta \mathbf{Y}_i}^{-1} \frac{\partial \mathbf{R}_{\Delta \mathbf{Y}_i}}{\partial \sigma_{\mu}} \mathbf{R}_{\Delta \mathbf{Y}_i}^{-1} \right) \right].$$

The estimation variance Cramer-Rao lower bound is

$$\sigma_{\sigma}^2 = 1 / \left(\mathbf{E} - \sum_{i=1}^v (\mathbf{B}_i^T \cdot \mathbf{F}_i^{-1} \cdot \mathbf{B}_i) \right). \quad (7)$$

Vector $\boldsymbol{\theta}_{\Sigma}$ is estimated according to iterative algorithm

$$\hat{\boldsymbol{\theta}}_{\Sigma}^{n+1} = \hat{\boldsymbol{\theta}}_{\Sigma}^n + \mathbf{F}_{\Sigma}^{-1} \big|_{\boldsymbol{\theta}_{\Sigma} = \hat{\boldsymbol{\theta}}_{\Sigma}^n} \cdot \boldsymbol{\Lambda}_{\Sigma} \big|_{\boldsymbol{\theta}_{\Sigma} = \hat{\boldsymbol{\theta}}_{\Sigma}^n}, \quad (8)$$

$$\hat{\sigma}_{\mu} = \hat{\boldsymbol{\theta}}_{\Sigma}(3 \cdot v + 1).$$

Initial approximation for the fBm parameters which are the part of $\hat{\boldsymbol{\theta}}_{\Sigma}^0$ is found at the first stage, the initial approximation for the variance is the estimation formed on previous iteration.

The estimate \hat{P}_{imp} has the form

$$\hat{P}_{imp} = \left(\sum_{t=1}^{m_{im}} \sum_{s=1}^{n_{im}} b_{\alpha}(t, s) - m_{im} n_{im} \alpha \right) / \left(\sum_{t=1}^{m_{im}} \sum_{s=1}^{n_{im}} k(t, s) - m_{im} n_{im} \alpha \right), \quad (9)$$

where $k(t, s) = (b - a) - (\min(\hat{x}_{pr}(t, s) + \sqrt{T_{\alpha} \cdot \sigma_{z-x}^2}, b) + \max(\hat{x}_{pr}(t, s) - \sqrt{T_{\alpha} \cdot \sigma_{z-x}^2}, a))$, matrix \mathbf{b}_{α} is computed according to (5) but with such threshold

$\mathbf{Y}(1) = y(t-1, s-1)$	•	$\mathbf{Y}(6) = y(t-1, s+1)$
$\mathbf{Y}(2) = y(t, s-1)$	$\mathbf{Y}(4) = y(t, s); x_0 = x(t, s)$	$\mathbf{Y}(7) = y(t, s+1)$
$\mathbf{Y}(3) = y(t+1, s-1)$	$\mathbf{Y}(5) = y(t+1, s)$	•

Fig. 2 Example of sample \mathbf{Y} forming

T_{α} that provides P_{fa} equal to α (this can be done by taking into account statistics of $T(t, s)$). The variance of \hat{P}_{imp}

$$\sigma_{P}^2 = \left(\sum_{t=1}^{m_{im}} \sum_{s=1}^{n_{im}} p_b(1 - p_b) \right) / \left(\sum_{t=1}^{m_{im}} \sum_{s=1}^{n_{im}} k(t, s) - m_{im} n_{im} \alpha \right)^2, \quad (10)$$

where $p_b = P_{imp} \cdot k(t, s) + (1 - P_{imp}) \cdot \alpha$.

4. EXPERIMENTAL RESULTS

Quantitatively the estimates $\hat{\sigma}_{\mu}^2$ are characterized by their bias

$\Delta = 100\% \cdot (\langle \hat{\sigma}_{\mu}^2 \rangle - \sigma_{\mu}^2) / \sigma_{\mu}^2$ and variance σ_{σ}^2 . The comparison has been performed to the recently proposed technique [6]. Since originally the method [6] has been proposed for additive noise variance estimation, one modification was introduced. Now original local estimates of σ_{μ}^2 are obtained as local estimates of variance divided by local squared means. The results of estimation for the standard test images are presented in Table 1. For fBm-algorithm ($N = 7$, $v = 1000$) both experimental (exp) and theoretical (theor) values of σ_{σ}^2 are given.

The analysis shows that for both methods the estimates are biased. This bias depends upon the test image and σ_{μ}^2 . However, for the fBm based algorithm, Δ and σ_{σ}^2 are significantly smaller than for the interquantile method (IQM) [6]. In comparison to IQM, the fBm-algorithm allows to reduce Δ by 5-26% and simultaneously to reduce σ_{σ}^2 by 2.5...4 times.

The experimental and theoretical values of σ_{σ}^2 for the proposed method coincide well enough to predict the method accuracy. This allows using theoretical variances σ_{σ}^2 to characterize estimation algorithm quality avoiding intensive computations for estimating experimental variances. For $v = 5300$ (maximal number of non-overlapping SWs) the variance σ_{σ}^2 is reduced by almost 6 times.

Quantitative results for joint estimation of σ_{μ}^2 and P_{imp} ($a = 0$, $b = 255$, $N = 7$, $v = 400$) are presented in Table 2. In our experiments, we set $T_{\alpha} = 20.25$. The analysis of these data demonstrates that the estimates of \hat{P}_{imp} are very close to the true values.

Experimental and theoretically predicted values of σ_p^2 and σ_σ^2 coincide well again. This allows pre-estimating (forecasting) the method accuracy from a given noisy image under interest.

One item is worth noting. The values σ_σ^2 and σ_p^2 are only the rough estimates of Cramer-Rao lower bound because of assumptions used in algorithm design as well as due to differences of real image and noise properties from the models used.

When P_{imp} increases, the efficiency of IQM reduces. The estimates $\hat{\sigma}_\mu^2$ become biased; the variance of $\hat{\sigma}_\mu^2$ significantly increases. Thus, the IQM is practically inoperative when $P_{\text{imp}}=10\%$.

In contrast to this method, for fBm-algorithm the bias and variance of estimate of $\hat{\sigma}_\mu^2$ slightly depend upon P_{imp} .

CONCLUSIONS

A novel method for joint estimation of multiplicative noise variance and probability of impulse noise occurrence has been designed. It possesses the following advantages: 1) applicability to textured images, 2) appropriate accuracy of obtained estimates of mixed noise parameters, 3) possibility to predict the method accuracy for processed noisy images.

Table 1. Experimental results of multiplicative noise variance estimation

Algorithm		$\sigma_\mu^2=0$		$\sigma_\mu^2=0.0025$		$\sigma_\mu^2=0.01$	
		$\langle \hat{\sigma}_\mu^2 \rangle$	σ_σ^2 (exp/theor)	$\Delta \%$	σ_σ^2 (exp/theor)	$\Delta \%$	σ_σ^2 (exp/theor)
Standard test image "Barbara"	IQM	0.00022	----	19.18	$(3.78/---) \cdot 10^{-9}$	7.48	$(4.20/---) \cdot 10^{-8}$
	fBm	$6.04 \cdot 10^{-5}$	$-/8.14 \cdot 10^{-12}$	8.28	$(1.50/1.13) \cdot 10^{-9}$	2.47	$(1.42/1.17) \cdot 10^{-8}$
Standard test image "Lena"	IQM	0.0002	----	13.26	$(2.45/---) \cdot 10^{-9}$	4.57	$(3.12/---) \cdot 10^{-8}$
	fBm	$8.38 \cdot 10^{-5}$	$-/4.60 \cdot 10^{-12}$	4.55	$(5.64/6.97) \cdot 10^{-10}$	-0.86	$(7.78/7.78) \cdot 10^{-9}$
Standard test image "Baboon"	IQM	0.00105	----	54.21	$(1.25/---) \cdot 10^{-8}$	21.16	$(1.11/---) \cdot 10^{-7}$
	fBm	$1.02 \cdot 10^{-4}$	$-/2.67 \cdot 10^{-10}$	27.24	$(3.60/3.03) \cdot 10^{-9}$	16.30	$(3.62/2.19) \cdot 10^{-8}$

Table 2. Joint estimation of σ_μ^2 and P_{imp} ("Baboon", $\sigma_\mu^2=0.01$)

	P_{imp}	\hat{P}_{imp}	$\sigma_p^2, \%$ (exp/theor)	$\Delta \%$	$\sigma_\sigma^2 \cdot 10^8$ (exp/theor)
fBm	0%	$\hat{P}_{\text{imp}} = P_{\text{imp}} = 0$		6.08	6.95/3.79
fBm	0%	0.04%	0.028/0.032	6.51	4.35/4.06
IQM	0%	---	---	10.87	33.0/----
fBm	5%	5.14%	0.28/0.36	9.42	6.50/4.38
IQM	5%	---	---	20.23	80.0/----
fBm	10%	9.90%	0.44/0.50	6.56	7.08/4.40
IQM	10%	---	---	202.42	19100/--

REFERENCES

- [1] *Advances in Environmental Remote Sensing*, Edited by F.M. Danson and S.E. Plummer, John Wiley & Son Ltd, 1995.
- [2] M.-P. Carton-Vandecandelaere, B. Vozel, L. Klaine and K. Chehdi, "Application to Multispectral Images of a Blind Identification System for Blur, Additive, Multiplicative and Impulse Noises," *Proc. of EUSIPCO*, France, V. III, pp. 283-286, 2002.
- [3] B. Vozel, K. Chehdi, L. Klaine, V.V. Lukin and S.K. Abramov, "Noise identification and estimation of its statistical parameters by using unsupervised variational classification," *Proceedings of ICASSP*, Toulouse, France, vol II, pp 841-844, 2006.
- [4] V.V. Lukin, S.K. Abramov, A.A. Zelensky and J. Astola, "Blind evaluation of noise variance in images using myriad operation," *Proceedings of IS&T/SPIE Int. Conf. on Image Processing: Algorithms and Systems*, USA, SPIE V. 4667, pp. 192-203, 2002.
- [5] V.V. Lukin, S.K. Abramov, B. Vozel and K. Chehdi, "A method for blind automatic evaluation of noise variance in images based on bootstrap and myriad operations," *Proceedings of SPIE/EUROPTO Symp. On Satellite Remote Sensing*, Bruges, Belgium, SPIE Vol. 5982, pp. 299-310, 2005.
- [6] V.V. Lukin, S.K. Abramov, A.A. Zelensky and J.T. Astola, "Use of minimal inter-quantile distance estimation in image processing," *Proceedings of SPIE Conference on Mathematics of Data/Image Pattern Recognition, Compression, and Encryption with Applications IX*, USA, SPIE Vol. 6315, 12 p, 2006. (in print)
- [7] V.V. Lukin, P.T. Koivisto, N.N. Ponomarenko, S.K. Abramov and J.T. Astola, "Two-stage Methods for Mixed Noise Removal", *CD-ROM Proceedings of EURASIP Workshop on Nonlinear Signal and Image Processing*, Japan, 6 p., 2005.
- [8] M. L. Uss, V. V. Lukin, I. V. Baryshev, B. Vozel and K. Chehdi, "Joint Estimation of Additive and Impulsive Noise Parameters in Remote Sensing Images with Fractal Structure," *Proc. of "Modern Problems of Radioengineering, Telecommunications and Computer Science"*, Ukraine, pp. 232-235, 2006.
- [9] A. P. Pentland, "Fractal-Based Description of Natural Scenes," *IEEE Tr. PAMI*, Vol.6, No.6, pp. 661-675, Nov. 1984
- [10] B.B. Mandelbrot, J. W. Van Ness, "Fractional Brownian motions, fractional noises and applications," *SIAM Rev.*, Vol. 10, pp. 422-437, 1968.
- [11] E. Abreu, M. Lightstone, S. K. Mitra, and K. Arakawa, "A new efficient approach for the removal of impulse noise from highly corrupted images," *IEEE Trans. Image Processing*, vol. 5, pp. 1012-1025, June 1996.
- [12] Uss M.L., "Filtering of images with fractal structure embedded in additive and impulsive noise," *Radiotekhnika*, Kharkov (Ukraine), Iss. 140, p. 57-69, 2005. (in Russian).
- [13] Uss M. L., "Filtering of images with fractal structure embedded in multiplicative noise," *East-European Journal of Advanced Technology*, № 2/2 (14), p. 127-132, 2005. (in Russian)